THE *IN-SILICO* OPTIMIZATION OF A BATCH REACTOR IN THE 2ND STEP OF CETUS PROCESS FOR D-FRUCTOSE PRODUCTION

Daniela GHEORGHE[1], Gheorghe MARIA*[2], Cristiana Luminita GÎJIU [3], Laura RENEA[4]

*Cetus technology is a well-known two steps enzymatic conversion of D-glucose to D-fructose with a high yield and selectivity. In the first step, a commercial pyranose 2-oxidase (P2Ox) is used to catalyze the oxidation of beta-D-glucose to keto-glucose (kDG). To avoid the fast P2Ox inactivation by the in-situ produced H_2O_2, catalase is added to decompose the continuously produced hydrogen peroxide. In the second Cetus step, kDG is reduced to D-fructose by using a commercial (recombinant human) aldose reductase (ALR) as biocatalyst, and NADPH as a donor of protons. A kinetic model of this 2-nd enzymatic step, adopted from literature, allowed optimization of the used batch reactor (**BR**). The **BR** optimal initial load is determined by using a nonlinear programming (**NLP**) procedure seeking for the D-fructose production maximization. Application of the Pareto optimal front technique (with considering multiple opposed objectives), proved to also offer a promising optimal operation of the analysed **BR**.*

Keywords: keto-glucose reduction to fructose; aldose reductase; kinetic model; NADPH; batch reactor; production maximization; Pareto optimal front

1. Introduction

Recent advances in obtaining genetically modified enzymes allowed developing a lot of biosynthesis of industrial interest, which tend to replace the classical fine chemical synthesis processes, due to the advantages of the enzymatic processes: a) produce fewer by-products; b) consume less energy; c) generate less environmental pollution; d) use smaller catalyst concentrations and much moderate reaction conditions [1].

[1] PhD student, eng., National University of Science and Technology POLITEHNICA Bucharest, Romania.
[2]* Acad. Professor PhD eng., National University of Science and Technology POLITEHNICA Bucharest, Romania; corresponding author: e-mail: gmaria99m@hotmail.com
[3] PhD eng., National University of Science and Technology POLITEHNICA Bucharest, Romania.
[4] PhD student, eng., National University of Science and Technology POLITEHNICA Bucharest, Romania.

However, to optimally solve the associated engineering problems (process design, operation, control, and optimization) it is essential to know an adequate mathematical (kinetic) model of the process. This model should preferably be based on the process mechanism, to ensure interpretable predictions of the process behavior under variable running conditions, easy to be compared with the literature data [2-4].

Despite their larger volumes, enzymatic reactors operated in **BR** (batch), or **FBR** (fed-batch) modes, are the most used because they ensure a high diffusion rate of compounds in the liquid phase, and an easy control of temperature/pH.

Concerning the reactor, an essential engineering problem refers to the development of *optimal operating policies* seeking for production maximization, raw-material consumption minimization, with obtaining a product of high quality (less by-products). This problem depends on the 1) adopted technology (chemical, biochemical, or biological catalysis), but 2) also on the used of engineering analysis to optimize the reactor operation (this paper).

In the **BR** case, its optimal operation problem can be ***in-silico*** solved in two alternatives: ***(a)*** **off-line** ('run-to-run'), the optimal operating policy being determined by using an adequate deterministic kinetic model previously identified based on experimental data (this paper; [5-12]); **(b)** ***on-line***, by using a simplified, often empirical mathematical model to obtain a state-parameter estimator based on the on-line recorded data (such as the classical Kalman filter) [9,13-20].

Even if the enzymatic process kinetic model is known, *in-silico* solving this off-line engineering problem is not an easy task, due to multiple contrary objectives, and a significant degree of uncertainty of the model/constraints [13,21]. The reactor optimal operating policy is usually determined by using an effective optimization rule [10,14,22-24]. In the deterministic alternative (this paper), single-/multi-objective criteria, including the product selectivity / yield maximization, (raw-)materials consumption minimization, are usually used to get feasible optimal operating strategies for the analyzed reactor [21] by using specific numerical algorithms [11,15,20,25].

Typical optimization objective functions were reviewed by [26,27]. The a-priori ***in-silico*** analysis allows comparing performances of various bioreactor constructive / operating alternatives, as follows [23].

BRs are commonly used for slow processes, because they are highly flexible and easy to operate in various alternatives [23]: ***(i).-*** simple **BR**, when substrate(s), biocatalyst, and additives initially loaded in recommended amounts [28-30]. Usually, a single- or multi-objective **BR** optimization is *off-line* performed to determine the best batch time, and substrate/biocatalyst initial load [13,16,22,30,31-35]; ***(ii).-*** a batch-to-batch (**BR**-to-**BR**) optimization, by including a model updating step based on acquired information from the past batches to determine the optimal load of the next **BR** [6-8,14,25,36-38]; ***(iii).-*** a sequence of

BRs of equal volumes linked in a series (**SeqBR**) [38]. For every **BR,** its content is transferred to the next one, with adjusting the reactants and biocatalyst concentrations of the latter, at *off-line* determined levels, to ensure its optimal operation [8,25]. ***(iv).-*** The **S**emi-**B**atch **R**eactor (**SBR)** or fed-batch reactor (**FBR),** with an optimally varied feeding policy of biocatalyst/substrate(s) is not discussed here [21,23,37,39]. Despite the **FBR**s better performances, they are difficult to operate, because they need previously prepared stocks of biocatalyst, and substrate(s), of different concentrations (a-priori *in-silico* determined), to be fed for every 'time-arc' of the batch (that is a batch-time equal division in which the feeding composition is constant) [23,24,40,41]. The time-step-wise variable optimal feeding policy of the **FBR** are determined *off-line* [23], or *on-line* [19].

D-fructose is a sweetener of high value in the food industry and medicine. As other polyols largely used as sweeteners (e.g. sorbitol, mannitol, xylitol, erythritol), it is produced on a large scale by using chemical or biochemical catalysis [42,43]. However, the chemical catalysis (that is hydrogenation of glucose on Ni, Fe, or Fe-Ni alloy catalysts) presents the critical disadvantage of significant energy consumption, occurring at high pressures (30 bar) and temperatures (140°C). One alternative is the beta-D-glucose isomerization to D-fructose on Fe/CarbonBlack catalyst [43]. Similarly, starting from the high-fructose syrup (HFCS) obtained from starch [44], after rough/fine filtration, ion exchange, and evaporation, a beta-D-glucose isomerization step leads to a high fructose syrup (HFS, of 42-55% D-fructose) [44-47].

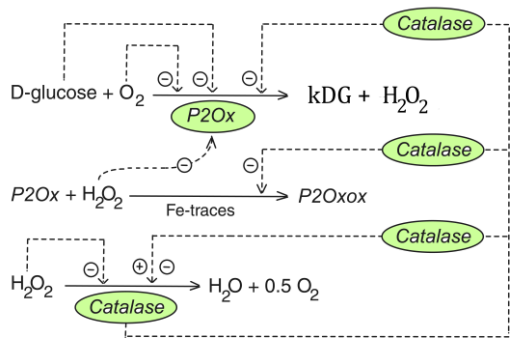

Step no. 1

Fig. 1. A simplified representation of the reaction pathway for beta-D-glucose enzymatic oxidation to kDG (D-glucosone) by using PO2x and catalase, proposed by Maria et al. [48]. Perpendicular dash arrows indicate the catalytic activation [+], repressing or inhibition [-] actions. Adapted from [48,49].

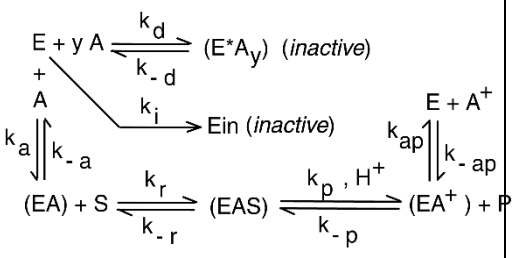

Step no. 2

Fig. 2. A simplified representation of the reaction pathway proposed by Maria and Ene [50] for keto-D-glucose (kDG) enzymatic reduction to D-fructose, by using NADPH and ALR. Notations are given in the abbreviation list. Adapted from [50], with the courtesy of CABEQ Jl.

By far, the biocatalytic route to produce D-fructose is more convenient due to a large number of advantages: it consumes less energy; by occurring at ambiental conditions, it produces less waste due to its high yield and selectivity, the product being free of allergenic compounds.

The two-step Cetus process for production of high purity D-fructose with high yields, are the followings [51,52]:

STEP 1).- Beta-D-glucose is firstly converted to kDG in the presence of pyranose 2-oxidase (P2Ox) at 25-30ºC and pH=6-7, with a high conversion and selectivity [48,49]. Catalase is added to decompose the resulted H_2O_2 (**Fig. 1**), thus avoiding the quick P2Ox inactivation. More details are given by [49,53,54].

STEP 2).- The kDG (D-glucosone) is then reduced to D-fructose by using a commercial (recombinant human) aldose reductase (ALR) (EC 1.1.1.21), and NAD(P)H as co-factor (proton donor), at 25ºC and pH=7 [50]. The resulted $NAD(P)^+$ will be continuously regenerated (*in-situ* or externally) and re-used [55-57] (**Fig. 2**). According to our results, the use of NADH instead of NADPH is preferable because NADPH deactivates very quickly, and it is more expensive than NADH [55]. The co-factor (NADPH or NADH) regeneration can be done in several ways [29,55,58-61]. For instance, Gijiu et al. [62] took this step, using the *in-situ* version, at the expense of the enzymatic degradation of ammonium formate [62]. More details about this process are given by [50].

This paper is aiming at optimizing the STEP-2 of the Cetus process, which is the kDG reduction to D-fructose (**Fig. 2**).

Thus, by adopting an adequate kinetic model from the literature the *in-silico* analysis will evaluate and compare the performances of several optimal operating policies of a **BR**. The **BR** optimal initial load will be determined by using a nonlinear programming (**NLP**) procedure seeking for the D-fructose production maximization in the presence of various technological constraints to limit de raw-materials consumption. Alternatively, the derived **Pareto-optimal fronts** (by considering multiple opposed objectives), proved to also offer a promising optimal operation policy of the analyzed **BR**.

The paper presents a significant number of novelty aspects, as following: ***(i)*** The engineering evaluation of this process is a premiere in the literature. ***(ii)*** The way by which this difficult multi-objective optimization problem was successfully solved is a model that can be followed to solve similar enzymatic processes. ***(iii)*** The present engineering analysis can be easily exploited in the development of this process (reactor design, control). ***(iv)*** The *in silico* (model-based) engineering analysis of a complex enzymatic process, leading to obtain a Pareto-optimal operating policy of the approached **BR** is an approach seldom used in the literature. ***(v)*** Confirmation that the Pareto-front 'break-point' choice proposed technique reported "fairly good" performances for a **BR**, from a multi-objectives' perspective. ***(vi)*** Before this paper, there are very few enzymatic

processes analyzed in the literature from the engineering point of view by also accounting the cofactor during the optimization procedure. ***(vii)*** The scientific value of this paper is not *virtual*, as long as the numerical analysis is based on the kinetic model of Maria and Ene [50] constructed and validated by using the extensive experimental data sets of (**Fig. 7**). ***(viii)*** The *in-silico* analysis suggests that an optimally operated **BR** with a policy determined from applying a NLP procedure, or the Pareto-optimal 'break-point' technique of [63-67] can lead to high performances.

2. The experimental enzymatic reactor

The analyzed **BR** here is those used by Maria [48,49] to derive the kinetic model of the Cetus first-step-process, and by Maria and Ene [50] to derive the kinetic model of the Cetus second-step process. The **BR** characteristics are presented in **Table 1** [68]. The reactor operation is completely automated, with a tight control of the dissolved oxygen (DO) concentration (for the oxidative processes, or for biological ones), of the pH, temperature, and of the mixing intensity [69].

In the **BR** operation mode, an optimal initial load will be determined by solving an optimization problem (product maximization here) in the presence of multiple technological constraints.

3. Bioprocess kinetics and bioreactor dynamic model

To model the dynamics of the key-species in the **BR,** a classical simple model was adopted, of ideal type [70], developed with the following main hypotheses: ***(i)*** Isothermal, iso-pH; ***(ii)*** The liquid phase is perfectly mixed (with no concentration gradients), by using continuous mechanical mixing. ***(iii)*** The liquid volume is quasi-constant, its increase due to the pH controlling additives being negligible.

Table 1.

Nominal (not-optimal) operating conditions (SPBR) of the experimental BR with suspended ALR and NADPH used to investigate the kDG conversion to D-fructose, by Maria and Ene [50]. DSn = data set number "n". Notations: [S = substrate (kDG); P = product (D-fructose); A = NADPH; A(+) = $NADP^+$; E = ENZ= ALR]

Parameter	Nominal initial value	Remarks
[S]o = [kDG]o	DS1, DS2, and DS3 (35 mM); DS4 (15 mM)	To be optimized within imposed limits (this paper)
[A]o = [NADPH]o	DS1, DS2, and DS4 (35 mM); DS3 (6 mM)	

[E]o = [ALR]o	DS1 (0.0048 U/mL), DS3 (0.0055 U/mL) DS2 (0.00257 U/mL) DS4 (0.006 U/mL)	
[P]o (D-fructose)	0	Final [P] is to be maximized
[A(+)]o = [NADP(+)]o	0	
[EA]o	0	
Temperature, pH (buffer)	25°C, 7	
Optimization tight limits (OTL), (mM)	[S]o ∈ [5-50]; [NADPH]o ∈ [5-50]; [E]o ∈ [0.003-0.1] [50]	
Optimization wide limits (OWL), (mM)	[S]o ∈ [5-100]; [NADPH]o ∈ [5-80]; [E]o ∈ [0.003-0.1] [50]	
Reactor volume	1 L (up to 3 L capacity)	
Batch time (tf)	24-76 h	DS1, DS2, DS4 (24 h); DS3 (24-76 h)
Beta-D-glucose (or kDG) solution solubility	Solubility 5-7M (25-30°C)	[71]
Beta-D-glucose (or kDG) solution viscosity	Ca. 1-3 cps (for up to 300 mM) 1000 cps (4.5M, 30°C), Vs. 1094 cps (molasses, 38°C)	[72] Wikipedia (molasse), 2024

The enzymatic **BR** dynamic model is presented in Eq.(1) with including the mass balances of 6 key-species of the process, that is (**Fig. 2**): [S = substrate (kDG); P = product (D-fructose); A = NADPH; A(+) = $NADP^+$; E = ENZ= ALR, E^*A], most of them being observable, with a measurable concentration.

$$\frac{dC_i(t)}{dt} = \pm r_i(\boldsymbol{C_o}, \boldsymbol{k}, t)\ ;\ C_{i,o} = C_i(t=0) \qquad \textbf{(1)}$$

Where ***Co*** is the vector of initial concentrations; ***k*** = rate constants vector. Species index "i" = [kDG, P, NADPH, NADP(+), ALR, E*A].

The process kinetic model is that proposed by Maria and Ene [50], based on the adopted reaction pathway of **Fig. 2**. The overall main reaction of **Table 2**, that is $\boldsymbol{r_P}$, follows a successive Bi-Bi mechanism. The reaction rate expressions, and the associated 9 rate constants are those identified by Maria and Ene [50].

Table 2.

The overall reactions considered by the kinetic model of Maria and Ene [50] (with the reaction scheme of Fig. 2) for (kDG) reduction to D-fructose by using commercial recombinant ALR (obtained by expressing human 1-316aa plasmids in *E. coli*; enzyme source: ATGEN, Cat. no. ALR-0901).

Overall reactions:

$$C_6H_{10}O_6\ (S) + \text{NADPH}\ (A) + H^+ \xrightarrow[\text{(phosphate buffer)}]{\text{ALR}\,(E),\ r_P}$$

$$C_6H_{12}O_6\ (P) + \text{NADP}^+\ (A^+)$$

$$y\,\text{NADPH} + \text{ALR} \underset{k_{-d}}{\overset{k_d}{\rightleftarrows}} (\text{ALR} \bullet \text{NADPH}_y)$$

$$\text{ALR}\ (E) \xrightarrow{r_i} \text{inactive ALR}\ (Ein)$$

Rate expressions (see also the reaction scheme of Fig. 2). Successive Bi-Bi mechanism.

$$r_d = k_d[A][E]\ ;\ r_{-d} = k_{-d}[E^*A]\ ;\ r_i = k_i[E]$$

$$K_A = \frac{[E][A]}{[EA]} = \frac{k_{-a}}{k_a}\ ;\ K_R = \frac{[EA][S]}{[EAS]} = \frac{k_{-r}}{k_r}\ ;\ K_{eq} = \frac{[EA^+][P]}{[EAS]} = \frac{k_p}{k_{-p}}\ ;$$

$$K_{AP} = \frac{[E][A^+]}{[EA^+]} = \frac{k_{ap}}{k_{-ap}}$$

An extensive and reasoned/documented discussion regarding derivation of this complex kinetic model starting from the reaction pathway of (**Fig. 2**) is given by Maria and Ene [50], and it is not repeated here.

The overall reduction reaction r_P of **Table 2** is thus obtained, being accompanied by a reversible binding of ALR to the NADPH to form an inactive complex (E^*A_y), and by the enzyme ALR deactivation. To estimate the 9 rate constants of this kinetic model (not given here), Maria and Ene [50] conducted a set of four batch experiments, presented in **Fig. 3**. To maximize the obtained kinetic information, these runs were carried out for large batch times of 24-76 h, and by varying the enzyme/reactant/cofactor initial ratios, in the range of: kDG $\in$ [15-35] mM; NADPH $\in$ [6-35] mM; ALR $\in$ [0.0026-0.006] U/mL.

The model rate constants have been estimated from using these four sets of experimental kinetic curves (**Fig. 3**). A weighted least square criterion has been used as statistical estimator, because the standard measurement error of species are very different [73]. The obtained kinetic model by Maria and Ene [50] was proved to be very adequate, the model predictions being in a fair agreement with the experimental data (**Fig. 3**). More details about the estimation step, and on the estimate statistical quality tests are given by Maria and Ene [50].

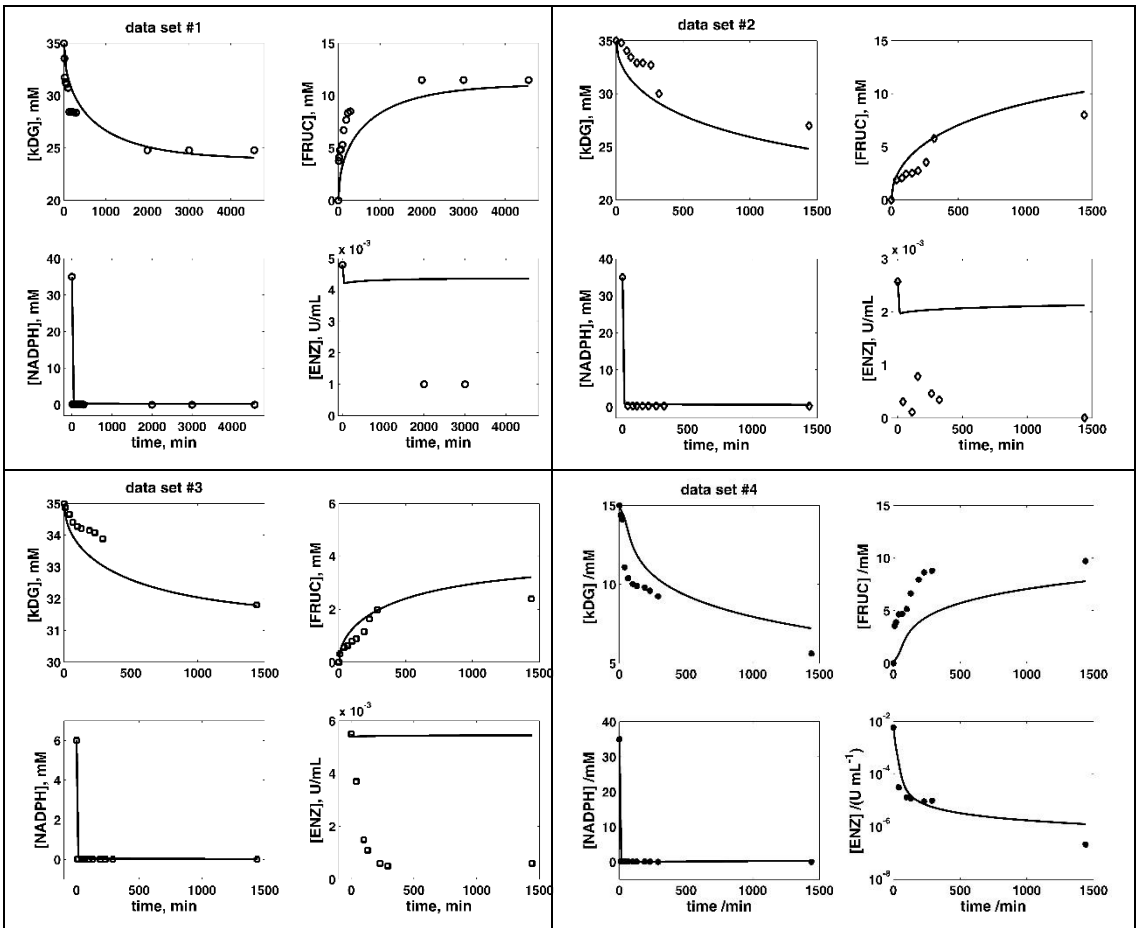

Fig. 3. Comparison of the kinetic model predictions (continuous line), vs.- the eperimental kinetic data (circles). Species dynamics concerns the observable species concentrations, that is for kDG(S), NADPH, D-fructose (P), and the enzyme E (suspended ALR). The initial conditions are the followings (phosphate buffer, pH = 7; 25ºC):
Data set # 1 - 35 mM kDG, 35 mM NADPH, 0.0048 U/mL ALR;
Data set # 2 - 35 mM kDG, 35 mM NADPH, 0.00257 U/mL ALR;
Data set # 3 - 35 mM kDG, 6 mM NADPH, 0.0055 U/mL ALR;
Data set # 4 - 15 mM kDG, 35 mM NADPH, 0.006 U/mL ALR.

4. BR optimization problem

4.1. Control variables selection

By analyzing the process main reactions of **Table 2, Fig.2**, the chosen control variables are those related to the reactor initial load.

4.2. Single objective function optimization (NLP)

Optimization of the **BR** operation translates in finding its initial load with the key-species [S]o = [KDG]o, [A]o = [NADPH]o, [E]o = [ALR]o (that is 3 unknowns here). In the present case, for a single objective function, this optimization problem can be referring to maximization of the [**P**] (D-fructose) production, that is:

Find [KDG]o, [NADPH]o, [ALR]o, such that: Max **Ω,** where: **Ω = [***P*(***C***(*t*),***C*****ₒ**,***k***)(*t*)**]**	**(2)**

The problem Eq. (2) can be solved by using a common nonlinear programming (**NLP**) optimization rule [3,73,74], seeking to determine the extreme of the objective function in the presence of multiple constraints**.**

In Eq. (2), the time-varying P(*t*) is in fact a multi-variable function *P*(***C***(*t*), ***C*****ₒ**,***k***)(*t*), evaluated by using the process/reactor model Eq. (1) over the whole batch time (*t*) ∈ [0, t_f], with the initial condition of $C_{j,0} = C_j(t=0)$ searched during optimization iterative numerical rule**.**

Because the enzymatic process kinetic model Eq. (1)**,** the optimization objective Eq. (2)**,** and the problem constraints Eq. (4) are all highly nonlinear, the formulated problem Eq. (2) translates into a difficult NLP with a multimodal objective function and a non-convex searching domain. To obtain the global feasible solution with enough precision, the multi-modal optimization solver MMA of Maria [73-75] has been used, being proved to be very effective for solving such difficult NLP problems.

4.3. Multi-objective optimization by using the Pareto optimal front

When more than one objective function are simultaneously considered, the optimization problem is more difficult to be solved. For multi-objective optimization, several alternatives can be followed [76,77]. One elegant option is to obtain a set of Pareto-optimal solutions, called Pareto-optimal front for the case of at least two adverse objectives [78]. A Pareto solution is one where any improvement in one objective can only take place at the cost of the other objective. For the present case study of **BR** optimization, several opposite objectives can be considered, such as: Max. P(D-fructose) production; Min. substrates [kDG] consumption; Min. co-factor [NADPH] consumption; Min. enzyme E (ALR) consumption. Of course, the Pareto-optimal fronts can be obtained by using any pair of these opposite objective functions. In the present paper, the following three Pareto-optimal fronts have been considered, by taking the above objectives two-by-two:

Max. P production –vs.- Min. substrate (kDG) consumption (initially added); Max. P production –vs.- Min. minimum NADPH consumption (initially added);	**(3)**

Max. P production –vs.- Min. minimum enzyme E (ALR) consumption (initially added).	

The rough Pareto-optimal fronts have been generated by using the dedicated algorithm (GAMULTIOBJ) of the MATLAB computational package. To be better interpreted, these rough Pareto-curves have been smoothed with using the cubic smoothing spline procedure CSAPS of Matlab.

4.4. Optimization problem constraints

The above formulated nonlinear optimization problem (**NLP**) Eq. (2), or the Pareto-optimal front problem Eq.(3), must account for the followings constraints:

(a).- The **BR** model Eq.**(1)**;

(b).- To limit the excessive consumption of raw-materials, feasible searching limits are imposed to the control/decision variable, in two alternatives:

(b1).- Large search intervals (**OWL** in **Table 1**).

(b2).- Tight search intervals (**OTL** in **Table 1**).

These feasible limits were based on the unpublished experimental information of Maria and Ene [50].

In a general form, the constraint **(b)** translates in the following relationships:

$$C_{i,o,min} \le C_{i,o} \le C_{i,o,max};\ \mathrm{i} = \mathrm{S, NADPH, E} \qquad \textbf{(4)}$$

5. Optimization results and their discussion

The **BR** optimization problem results are the following:

-.- The Pareto optimal fronts for several opposite objectives (**Figs. 4-6**);

-.- The **NLP** optimal operating policy comparatively displayed vs. experimental data set #1 in (**Fig. 7**);

-.- A comparison of all **BR** operating alternatives in terms of P production and raw-materials consumption (based on the initial load) in **Table 3.**

By analyzing these results, and the operating alternatives of **Table 3**, several conclusions can be derived, as follows:

(1).- In the Pareto optimal front case, four opposite objectives have been considered, according to Eq.(3). The most important Pareto-front is that indicating the dependence of the [maximum D-fructose production vs.- minimum substrate (kDG) consumption (initially added)] (**Fig. 4**). According to the suggestions of Maria [78-82], the slope "breakpoint" in the exponential-like increasing Pareto-curve can be considered as being the preferred solution of the optimization problem. However, the irregular increasing curve makes this option difficult. The chosen optimal set-point (SP) displayed in **Table 3** , at one of the "breakpoints" of

the curve of (**Fig. 4**) is that realizing a high P-productivity, with the same consumption of kDG and NADPH, as in the optimal **NLP** policy case. However, despite the "fairly good" performances of this Pareto-optimal SP, the enzyme consumption is 10x higher than in the optimal **NLP** case, making the **NLP** optimal policy to be preferred.

(2).- The nominal, not-optimal **BR** operation **SPBR** reported very poor performances in **Table 3**. The species dynamics trajectories during the batch time for the best **NLP** optimal operating policy of **BR** is given in **Fig. 7.** Compared to the experimental curves of the nominal, not-optimal **BR** operation (data set #1) the **NLP** optimal operation reported superior performances: 3x higher P-productivity, with 2x-3x higher consumption of (kDG, NADPH), but with a 60% less consumption of ALR.
Thus, the *in-silico*, *off-line* **BR** optimization of this paper appears to be fully justified by the obtained better operating policies.

(3).- By analyzing the **NLP** optimal operating policies of the **BR**, with using **OWL** vs. **OTL** search intervals for the control variables, and also the **Fig. 7** with the species dynamics in the best **NLP** operating case, some conclusions can be derived: a) the P-productivity increases with the initial substrates [kDG, NADPH] concentrations, if enough ALR is present, and if ALR does not deactivate too fast. To better fulfill such a condition, the best alternative appears to be the use of a more stable enzyme, that is immobilized on a suitable porous support [78-80]; b) The **NLP** optimally operated **BR** with large searching intervals (**OWL**) for the control variables reported much better performances (2x more in terms of produced P, and 2x less in terms of consumed kDG, NADPH) compared to the optimal **BR** by using tight searching intervals (**OTL**) in **Table 3**.

(4).- For a enough stable (immobilized) enzyme, the P(D-fructose) production maximization, clearly depends on the available amount of substrate (kDG) and cofactor (NADPH). As the kDG results from the step 1 of the Cetus process [48,49], a more realistic optimization must consider concomitantly the both linked Cetus process.

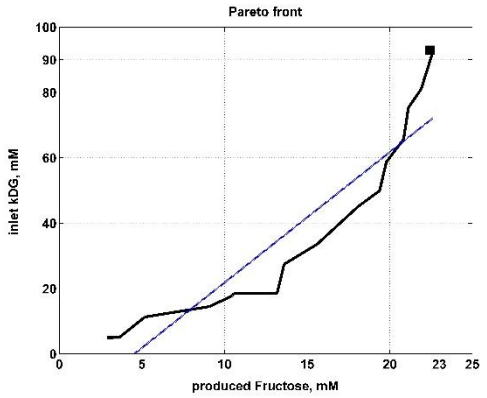

Fig. 4. The Pareto-optimal front in terms of Min. substrate (kDG) consumption (initially added)-vs.- Max. P(D-fructose) production, for **OWL** limits (**Table 1**) of control variables. The marked SP was chosen according to [63-67]. The blue line is the smoothed Pareto-optimal front.

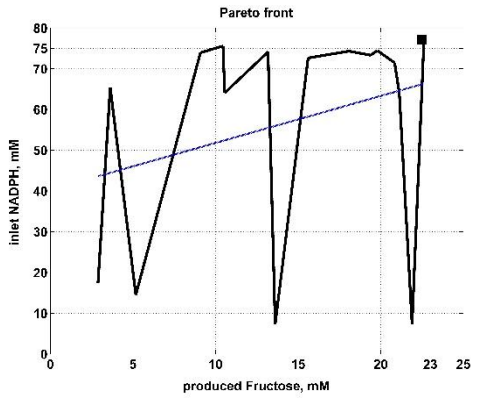

Fig. 5. The Pareto-optimal front in terms of Min. NADPH consumption (initially added)-vs.- Max. P(D-fructose), for **OWL** limits (**Table 1**) of control variables. The marked SP is the same as the one chosen in **Fig. 4**. The blue line is the smoothed Pareto-optimal front.

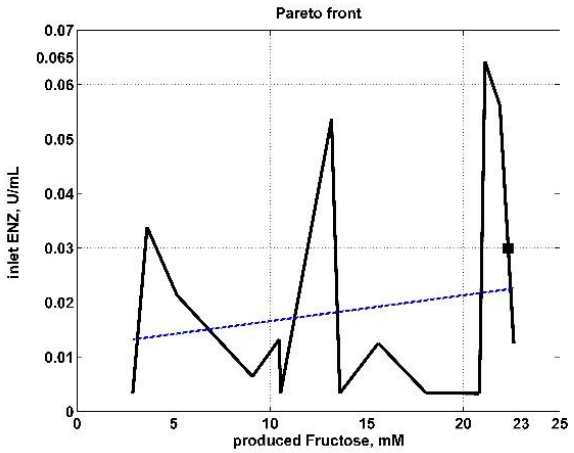

Fig. 6. The Pareto-optimal front in terms of Min. enzyme E consumption (initially added)-vs.- Max. P(D-fructose), for **OWL** limits (**Table 1**) of control variables. The marked SP is the same as the one chosen in **Fig. 4**. The blue line is the smoothed Pareto-optimal front.

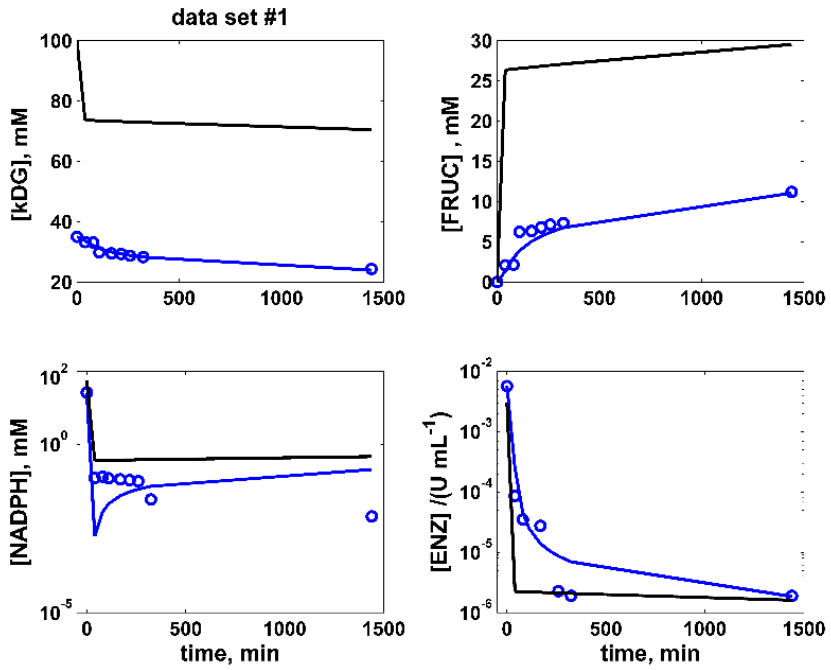

Fig. 7 [**Black line**] The *in-silico* determined **NLP** best optimal operating policy of the **BR** given in **Table 3**, in terms of the key-species dynamics over the batch time, with imposing the **(OWL)** optimization wide limits of **Table 1.** [**Blue line, and blue points**] The not-optimal operation of **BR** by Maria and Ene [50] in terms of experimental kinetic curves and data points for the same key-species of the enzymatic process, for the data set # 1 case.

6. Conclusions

To conclude, the *in-silico, off-line* optimized **BR** operation, even simple, can offer a significantly improved effectiveness, due to its high flexibility in using an easily adaptable process model [81], and due to the applied effective optimization rules (single objective **NLP**, and the multi-objective Pareto-fronts techniques).

The nominal, not-optimal **BR** operation **SPBR** reported very poor performances. Compared to this **BR** poor operation, the single/multi-objective optimal **BR** operation reported superior performances: 3x higher product-productivity, even if at the cost of a 2x higher consumption of raw-materials (kDG, NADPH, ALR). Thus, the *in-silico* **BR** optimization of this paper appears to be fully justified by the obtained better operating policies.

Table 3

BR productivity and raw-materials consumption when operated in various modes. The BR optimal policy compared to the experimental data set #1 is given in Fig. 7. The main characteristics of the BR are given in Table 1. The reactor volume is of 1 L in all cases.

Bioreactor operation				**Raw-material consumption (a,b)**			**D-fructose production, (b)**
BR policy	Obs.			kDG, mmoles	NADPH, mmoles	E (ALR) (U) (c)	(mmoles)
BR Experimental, Maria and Ene [50]	Not-optimal data set #1, Fig. 7	Nominal initial load SPBR (d,g)		35	35	4.8	11.05 (poor)
		[KDG]o	35				
		[NADPH]o	35				
		[ALR]o	0.0048				
BR NLP optimal initial load (this paper) (OWL)	(e) Fig. 7	Optimal load wide limits (OWL)		100	80	3.0	29.54 (best)
		[KDG]o	100				
		[NADPH]o	80				
		[ALR]o	0.003				
BR NLP optimal initial load (this paper) (OTL)	(f)	Optimal load tight limits (OTL)		48.73	48.75	3.1	15.1 (poor)
		[KDG]o	48.73				
		[NADPH]o	48.75				
		[ALR]o	0.0031				
BR Pareto-optimal initial load (this paper) (OWL)	(e-h)	Optimal load wide Limits (OWL)		100	80	33	29.54 (fairly good)
		[KDG]o	100				
		[NADPH]o	80				
		[ALR]o	0.033				

Footnotes:
(a) Referring to the reactor liquid initial volume of 1 L (**Table 1**).
(b) The displayed digits come from the numerical simulations.
(d) The **BR** experimental nominal set-point #1 (**Table 1, Fig.3**) of Maria and Ene [54]. Notation: **SPBR** = the **BR** nominal set-point; SP = set point.
(e). **BR** optimal policy (initial load) was obtained using larger search intervals (**OWL, Table 1**)
(f) **BR** optimal policy (initial load) was obtained using tight search intervals (**OTL, Table 1**)
(g) The units are: [kDG], mM; [NADPH], mM; [ALR], (U/mL).
(h) Search intervals used to obtain the optimal SP are those from (e).

Abbreviations and notations

c_j	-	Species *j* concentration, M
k_j, K_j, y	-	Rate constants (M, s, U/L units)
r_j	-	Reaction rate of species "*j*" (M/s, U/L.s)
t	-	Time (s)
Index		
0,o	-	Initial
A, A^+	-	NADPH, $NADP^+$
ALR	-	Aldose reductase
E, ENZ	-	Enzyme, that is the aldose reductase (ALR)
kDG, D-glucosone	-	2-keto-D-glucose
NAD(P)H	-	Nicotinamide adenine dinucleotide (phosphate) reduced form
OTL, OWL		Optimization tight / wide limits respectively
P	-	Product (fructose)
P2Ox	-	Pyranose 2-oxidase
P2Oxox	-	Inactive form of P2Ox
S	-	Substrate (kDG here)
SP	-	Set point (BR running conditions)

R E F E R E N C E S

[1].- *Moulijn, J.A., Makkee, M., van Diepen, A.*, „Chemical process technology", Wiley, New York, 2001.

[2].- *Vasić-Rački, D., Findrik, Z., Presečki, A.V.,* Applied Microbiology and Biotechnology **91**, 2011, pp. 845-856.

[3].- *Maria, G.,* Chem. Biochem. Eng. Q., **18**, 2004, pp. 195-222.

[4].- *Gernaey, K.V., Lantz, A.E., Tufvesson, P., Woodley, J.M., Sin, G.,* Trends in Biotechnology, **28**, 2010, pp. 346–354.

[5].- *Bonvin, D., Srinivasan, B., Hunkeler, D.*, IEEE Control systems magazine, Dec. 2006, pp. 34-45.

[6].- *Srinivasan, B., Primus, C.J., Bonvin, D., Ricker, N.L.,* Control Engineering Practice, **9**, 2001, pp. 911-919

[7].- *Dewasme, L., Amribt, Z., Santos, L.O., Hantson, A.L., Bogaerts, P., Wouwer, A.V.,* The International Federation of Automatic Control, **46**, 2013, pp. 60-65.

[8].- *Dewasme, L., Cote, F., Filee, P., Hantson, A.L., Wouwer, A.V*., Bioengineering (Basel), **4**, 2017, pp. 17.

[9].- *Mendes, R., Rocha, I., Pinto, J.P., Ferreira, E.C., Rocha, M.*, In: *Chakraborty, U.K.* (ed.), „Advances in differential evolution. Studies in Computational Intelligence", Springer verlag, Berlin, 2008, pp. 299-317.

[10].- *Liu, Y., Gunawan, R., J. Biotechnol.,* **244**, 2017, pp. 34-44.
[11].- *Hartig, F., Keil, F.J., Luus, R.,* Hung. J. Ind. Chem., **23**, 1995, pp. 81-160.
[12].- *Amribt, Z., Dewasme, L., Wouwer, A.V., Bogaerts, P.*, Bioprocess Biosyst Eng., **37**, 2014, pp. 1637–1652.
[13].- *Bonvin, D.,* J. Process Control., **8**, 1998, pp. 355-368.
[14].- *Bonvin, D.,* "Real-time optimization", MDPI, Basel**,** 2017**.**
[15].- *DiBiasio, D.,* In: "Chemical engineering problems in biotechnology"*, Shuler, M.L.* (ed.), AIChE publ., New York, 1989, pp. 351-391.
[16].- *Abel, O., Marquardt, W.*, J. Process Control., **13**, 2003, pp. 703-715.
[17].- *Lee, J., Lee, K.S., Lee, J.H. Park, S.*, Control Eng. Pract., **9**, 2001, pp. 901-909.
[18].- *Ruppen, D., Bonvin, D., Rippin, D.W.T.,* Comput. Chem. Eng., **22**, 1998, pp. 185-199.
[19].- *Loeblein, C., Perkins, J., Srinivasan, B., Bonvin, D.,* Comput. Chem. Eng., **21**, 1997, pp. S867-S872.
[20].- *Rao, M., Qiu, H.,* "Process control engineering: a textbook for chemical, mechanical and electrical engineers", Gordon and Breach Science Publ., Amsterdam, 1993.
[21].- *Smets, I.Y., Claes, J.E., November, E.J., Bastin, G.P., van Impe, J.F.,* J. Process Control., **14**, 2004, pp. 795-805.
[22].- *Srinivasan, B., Bonvin, D., Visser, E., Palanki, S.,* Comput. Chem. Eng., **27**, 2003, pp. 27-44.
[23].- *Maria, G.*, Molecules, **25**(23), 2020, 5648.
[24].- *Maria, G., Renea, L.,* Bioengineering-Basel, **8**, 2021, 210.
[25].- *Martinez, E.,* Proc. 2nd Mercosur Congress on Chemical Eng., Rio de Janeiro, Costa Verde, Brasil, **2005**, paper #20.
[26].- *Engasser, J.M.,* Chem. Eng. Sci., **43**, 1988, pp. 1739-1748.
[27].- *Scoban, A.G., Maria, G.,* Asia-Pacific J. Chem. Eng., **11**, 2016, pp. 721-734.
[28].- *Maria, G.,* Comput. Chem. Eng., **133**, 2020A, pp. 106628-106635.
[29].- *Wang, P.,* Appl. Biochem. Biotechnol.*,* **152**, 2009, pp. 343–352.
[30].- *Ozturk, S.S., Palsson, B.O.*, J. Biotechnol., **16**, 1990, pp. 259-278.
[31].- *Saha, B.C.; Racine, F.M.,* Appl. Microbiol. Biotechnol., **89**, 2011, pp. 879–891.
[32].- *Von Weymarn, N.,* PhD Diss., Helsinki University of Technology, Laboratory of Bioprocess Engineering, 2002.
[33].- *Song, K.H.; Lee, J.K.; Song, J.Y.; Hong, S.G.; Baek, H.; Kim, S.Y.; Hyun, H.H.,* Biotechnology Letters*,* **24**, 2002, pp. 9–12.
[34].- *Loesche, W.J.; Kornman, K.S.*, Arch. Oral Biol., **21**, 1976, pp. 551-553.
[35].- *Bäumchen, C.; Roth, A.H.F.J.; Biedendieck, R.; Malten, M.; Follmann, M.; Sahm, H.; Bringer-Meyer, S.; Jahn, D.,* Biotechnol. J., **2**, 2007, pp. 1408–1416.
[36].- *Lübbert, A., Jørgensen, S.B.,* J. Biotechnol., **85**, 2001, pp. 187-212.
[37].- *Binette, J.C., Srinivasan, B.,* Processes, **4**, 2016, pp. 27.
[38].- *Maria, G., Peptanaru, I.M.,* Dynamics-Basel-MDPI, ***1****,* 2021, pp. 134-154.
[39].- *Franco-Lara, E., Weuster-Botz, D.,* Bioprocess Biosyst. Eng., **28**, 2005, pp. 71-77.
[40].- *Maria, G., Dan, A.,* Comput. Chem. Eng., **35**, 2011, pp. 177-189.
[41].- *Avili, M.G.; Fazaelipoor, M.H.; Jafari, S.A.; Ataei, S.A.,* Iranian Journal of Biotechnology, **10**, 2012, pp. 263-269.
[42].- *Akinterinwa, O., Khankal, R., Cirino, P.C.,* Current Opinion in Biotechnology, **19**, 2008, pp. 461–467.
[43].- *Fu, Y., Ding, L., Singleton, M.L., Idrissi, H., Hermans, S.,* Applied Catalysis B: Environmental, **288**, 2021, pp. 119997.
[44].- Liese, A., Seelbach, K., Wandrey, C. (Eds), Industrial biotransformations, Wiley-VCH, Weinheim, 2006.
[45].- *Myande Comp.*, China, 2024,

[46].- *Marianou, A.A., Michailof, C.M., Pineda, A., Iliopoulou, E.F., Triantafyllidis, K.S., Lappas, A.A.,* ChemCatChem, **8**, 2016, pp. 1100-1110.
[47].- *Hanover, L.M., White, J.S.,* The American Journal of Clinical Nutrition, **58**, 1993, pp. 724S-732S.
[48].- *Maria, G., Ene, M.D., Jipa, I.,* Journal of Molecular Catalysis B: Enzymatic, **74**, 2012, pp. 209-218.
[49].- *Ene, M.D., Maria, G.,* Journal of Molecular Catalysis B: Enzymatic, **81,** 2012, pp.19-24.
[50].- *Maria, G., Ene, M.D., Chem. Biochem. Eng. Quarterly,* **27**, 2013, pp. 385–395.
[51].- *Leitner, C., Neuhauser, W., Volc, J., Kulbe, K.D., Nidetzky, B., Haltrich, D.,* Biocatal. Biotransform. **16**, 1998, pp. 365-382.
[52].- *Shaked, Z., Wolfe, S.,* Methods Enz. **137**, 1988, pp. 599-615.
[53].- *Williams, J.*, J Gen Physiol, **11**, 1928, pp. 309–337.
[54].- *Bastian, S., Rekowski, M., Witte, K., Heckmann-Pohl, D., Giffhorn, F.*, Appl Microbiol Biotechnol, **67**, 2005, pp. 654–663.
[55].- *Chenault, H.K.., Whitesides, G.M.,* Appl. Biochem. Biotechnol., **14,** 1987, pp. 147-197.
[56].- *Slatner, M., Nagl, G., Haltrich, D., Kulbe, K.D., Nidetzky, B.,* Biocatal. Biotransform., **16,** 1998, pp. 351-363.
[57].- *Parmentier, S., Arnaut, F., Soetaert, W., Vandamme, E.J.,* Biocatalysis and Biotransformation, **23,** 2005, pp. 1-7.
[58].- *Leonida, M.D.*, Current Medicinal Chemistry, **8** , 2001, pp. 345-369.
[59].- *Slatner, M., Nagl, G., Haltrich, D., Kulbe, K.D., Nidetzky, B.*, Annals New York Academy of Sciences **20** , 2002, pp. 450-453.
[60].- *Liu, W., Wang, P.,* Biotechnology Advances, **25** , 2007, pp. 369-384.
[61].- *Berenguer-Murcia, A., Fernandez-Lafuente, R.*, Current Organic Chemistry, **14,** 2010, pp. 1000-1021.
[62].- *Gijiu, C.L., Maria, G., Renea, L.*, Chemical Engineering and Technology, 2024, e202300555. doi: 10.1002/ceat.202300555
[63].- *Dan, A., Maria, G.***,** Chemical Engineering & Technology*,* **35**, 2012, pp. 1098-1103.
[64].- *Dan, A., Maria, G.*, Environmental Eng. and Management Journal, **12**, 2013, pp. 245-250.
[65].- *Dan, A., Maria, G.*, U.P.B. Sci. Bull., Series B – Chemistry and Materials Science, **76**, 2014, pp. 35-48.
[66].- *Muscalu, C., Maria, G.*, Revue Roumaine de Chimie, **61**, 2016, pp. 881-892.
[67].- *Maria, G., Khwayyir, H.H.S., Dinculescu, D.,* Chem. Biochem. Eng. Quarterly, **30**, 2016, pp. 279-290.
[68].- *Maria, G., Renea, L., Gheorghe, D.*, *Revue Roumaine de Chimie*, 2024, 69(5-6), 263-278.
[69].- *Chen, M.,* Ph.D. Thesis, TU Hamburg, Germany, 2020.
[70].- *Moser, A.*, „Bioprocess technology - kinetics and reactors", Springer Verlag, Berlin, 1988.
[71].- *Bishop, M.,* "An introduction to chemistry", Chiral publ., 2013. https://preparatorychemistry.com/Bishop_contact.html
[72].- *Laos, K., Harak, M.,* J. Food Physics, **27**, 2014, pp.27-30.
[73].- *Maria, G.,* "Analiza statistică şi corelarea datelor experimentale (bio)chimice. Repartiţii şi estimatori statistici", Printech, Bucharest, 2008, ISBN 978-973-718-886-1.
[74].- *Maria, G.,* In: „Modelling, identification and control", *Hamza, M.H.*(ed.), IASTED/ACTA Press, Anaheim (CA, USA), 2003, pp. 112-118.
[75].- *Maria, G.***,** In: *Pekny, J.F., Blau, G.E., Carnahan, B.* (Eds.), AIChE Symp. Series, **94**, no. 320, 1998, pp. 351-359.
[76].- *Rao, S.S.,* "Engineering optimization – Theory and practice", Wiley, New York, 2009. Chapter 14.10.[77].- *Nagrath, D., Avila-Elchiver, M., Berthiaume, F., Tilles, A.W., Messac, A., Yarmush, M.L.,* Metab Eng., **12**, 2010, pp. 429–445.

[78].- *Tanaka, A., Tosa, T., Kobayashi, T.* (Eds.), „Industrial applications of immobilized catalysts“, Marcel Dekkwer, New York, 1993.
[79].- *Bickerstaff, G.F.* (Ed.), “Immobilization of Enzymeas nd Cells”, Humana Press Inc., Totowa (New Jersey), 1997.
[80].- *Guisan, J.M.* (Ed.), “Immobilization of Enzymes and Cells”, Humana Press, Totowa, New Jersey, 2006.
[81].- *Fotopoulos, J., Georgakis, C., Stenger jr., H.G.,* Chem. Eng. Sci., **49**, 1994, pp. 5533-5547